

**Important note: The present paper work was sent to Engineering Structures on 23 April 2020 (it is currently under review).**

## **The Z-octahedron family: a new tensegrity family**

Manuel Alejandro Fernández-Ruiz<sup>a,\*</sup>, Enrique Hernández-Montes<sup>b</sup>, Luisa María Gil-Martín<sup>c</sup>

<sup>a</sup>Department of Industrial and Civil Engineering, University of Cádiz (UCA). Campus Bahía de Algeciras, Avda. Ramón Puyol, s/n. 11201 Algeciras (Cádiz), Spain. manuelalejandro.fernandez@uca.es.

\*Corresponding author

<sup>b</sup>Department of Structural Mechanics, University of Granada (UGR). Campus Universitario de Fuentenueva s/n. 18072 Granada, Spain. emontes@ugr.es.

<sup>c</sup>Department of Structural Mechanics, University of Granada (UGR). Campus Universitario de Fuentenueva s/n. 18072 Granada, Spain. mlgil@ugr.es.

### **Abstract**

A new family of tensegrity structures is presented: the Z-octahedron family. A tensegrity family is a group of tensegrity structures that share a common connectivity pattern. The members of the Z-octahedron family have been obtained replacing the elementary rhombic cells of the members of the octahedron family with elementary Z-shaped cells. In addition, a higher number of possible force density or force:length ratio values have been considered. The values of the force:length ratio of the members of the family that lead to super-stable tensegrity forms have been computed analytically. Two members of the family have been obtained: the Z-expanded octahedron and the Z-double-expanded octahedron. Finally it has been proved that the Z-double-expanded octahedron obtained here from topological rules can also be defined from a truncated cube based on purely geometrical intuition.

**Keywords:** Tensegrity; Z-Octahedron family; Octahedron family; Analytical form-finding; Force density method.

## 1. Introduction

Tensegrity structures were first introduced by Fuller [1]. They are pin-jointed free-standing pre-stressed structures composed of a set of compression (struts) and tension (cables) members that are self-equilibrated. Tensegrity structures have an extensive range of important and novel applications in many fields such as biology [2,3], aerospace engineering [4], robotics [5] and civil engineering [6,7] due to their light-weight, innovative forms and deployability. They have had a great development in recent years due to the growing interest in mechanical metamaterials [8].

Unlike conventional structural forms such as trusses and frames where the geometries are generally known, in the case of tensegrity structures its geometrical configuration and the prestress state of the members are interdependent with each other. The process of determining a suitable prestress state and its corresponding equilibrium shape is called form-finding. A review of form-finding methods of tensegrity structures can be seen in the work carried out by Tibert and Pellegrino [9]. The Force Density Method (FDM) proposed by Schek [10,11] is a form-finding method of pin-jointed structures originally conceived for tension structures. The FDM is present in several form-finding methods of tensegrity structures [12–14], and it is based on the concept of force:length ratio or force density  $q$ . Otter [15] presented the dynamic relaxation method which has also been used in the form-finding problem of tensegrity structures [16,17].

The existing form-finding methods can be generally classified into two categories: analytical and numerical. Analytical methods find the equilibrium shape of simple tensegrity forms with a high order of symmetry through a symbolic analysis (see [13,18–

20]). Regarding numerical methods, they can be applied to relatively complicated tensegrities with a high number of members or with lack of symmetry; examples of them can be seen in [12,14,21–23].

A tensegrity family is defined as a group of tensegrity structures that share a common connectivity pattern [20]. The octahedron family is a good example of tensegrity family [20]. The members of this family are: the octahedron, the expanded octahedron and the double-expanded octahedron. Each member of the family comes from the expansion of a previous member. In addition, each member of the family has as folded forms all the previous members of the family. Folded forms are tensegrity structures with nodes having the same coordinates (i.e. the nodes have the same position in the space) [18]. On the contrary, full forms are tensegrity structures all nodes have different coordinates one to one.

One of the main advantages of a tensegrity family is the possibility of defining new tensegrity forms based on topology rules. A tensegrity family can be considered as a source of new tensegrity forms that share the same connectivity pattern. On the other hand, there are other sources of tensegrity structures based purely on geometry as the tensegrity forms obtained from truncated regular polyhedrons [19,24,25].

In this work a new tensegrity family is defined: the Z-octahedron family. The members of the Z-octahedron family have been obtained replacing the elementary rhombic cells of the members of the octahedron family presented by [20] by elementary Z-shaped cells. The first two members of this presented family are the Z-expanded octahedron and the Z-double-expanded octahedron, both super-stable. The values of the force densities or force:length ratios that satisfy the super-stability conditions have been computed analytically for all the members of the Z-octahedron family.

## 2. Equilibrium, rank deficiency and super-stability of tensegrity structures

### 2.1 Equilibrium of tensegrity structures

The FDM [11] is a well-known form-finding method for general networks. A mesh is composed by  $n$  free nodes,  $n_f$  fixed nodes and  $m$  members. The difference between free and fixed nodes is that the former ones are free to move in the space while the latter ones have a fixed position (they act as supports). The connectivity between the nodes of the mesh is defined by the connectivity matrix  $\mathbf{C}_S \in \mathfrak{R}^{m \times (n+n_f)}$ . If a branch of the mesh  $j$  links nodes  $i$  and  $k$  (with  $i < k$ ),  $\mathbf{C}_S$  is defined as follows:

$$\mathbf{C}_S(j,r) = \begin{cases} +1 & \text{if } i(j) = r \\ -1 & \text{if } k(j) = r \\ 0 & \text{otherwise} \end{cases} \quad (1)$$

In Eq.(1)  $r$  denotes the  $r$ th column of the  $j$ th row in  $\mathbf{C}_S$ . Matrix  $\mathbf{C}_S$  must be known at the beginning of the form-finding procedure; Hernández-Montes et al. [26] proposed some topological rules in order to define  $\mathbf{C}_S$  for a general mesh.

Schek [11] proposed to number the fixed nodes at the end of the sequence. By doing so,  $\mathbf{C}_S$  can be partitioned into two matrices  $\mathbf{C} \in \mathfrak{R}^{m \times n}$  and  $\mathbf{C}_f \in \mathfrak{R}^{m \times n_f}$  ( $\mathbf{C}_S = [\mathbf{C} \ \mathbf{C}_f]$ ).

The equilibrium equations of the mesh are linearized by assigning specific values of force:length ratios  $q$  to each member of the mesh [10,11]. The force:length ratio is defined as the ratio between the axial force and the length of each member, and it is considered to be an input in the form-finding problem.

In tension structures [27] all the members are in tension, that corresponds with  $q > 0$ , and the self-weight is ignored (see Figure 1.e). On the contrary, in compression structures [28] all the members are in compression ( $q < 0$ ) and the self-weight is the dominant load (see Figure 1.d). Compression structures with tensions members (Figure 1.a) is a new type of structures recently introduced by the authors [29] composed by a compression structure and tensions members that connect two points of the compression structure. As

in the case of compression structures, self-weight cannot be ignored. Cable-strut structures (Figure 1.b) are pin-jointed structures composed by tension (cables,  $q > 0$ ) and compression members (struts,  $q < 0$ ). Special cases of cable-strut structures are cable domes [30,31] and cable-stiffened arches [32]. As in tension structures, the self-weight of cable-strut structures is usually ignored. Finally, tensegrity structures (Figure 1.c) are free-standing cable-strut structures, and so no supports exist. Taking all of the above into account, the equilibrium equations of tensegrity structures can be formulated as [11,12]:

$$\left. \begin{aligned} \mathbf{D} \cdot \mathbf{x} &= \mathbf{0} \\ \mathbf{D} \cdot \mathbf{y} &= \mathbf{0} \\ \mathbf{D} \cdot \mathbf{z} &= \mathbf{0} \end{aligned} \right\} \quad (1)$$

In Eq. (1)  $\mathbf{D}$  is the force density matrix, which is computed as  $\mathbf{D} = \mathbf{C}^T \mathbf{Q} \mathbf{C} \in \mathcal{R}^{n \times n}$  and  $\mathbf{x} = [x_1, \dots, x_n]^T$ ,  $\mathbf{y} = [y_1, \dots, y_n]^T$  and  $\mathbf{z} = [z_1, \dots, z_n]^T$  are the nodal coordinate vectors. Matrix  $\mathbf{Q} \in \mathcal{R}^{m \times m}$  is the diagonal square matrix of vector  $\mathbf{q} = [q_1, \dots, q_m]^T$ , which collects the force: length ratio of each member of the tensegrity.

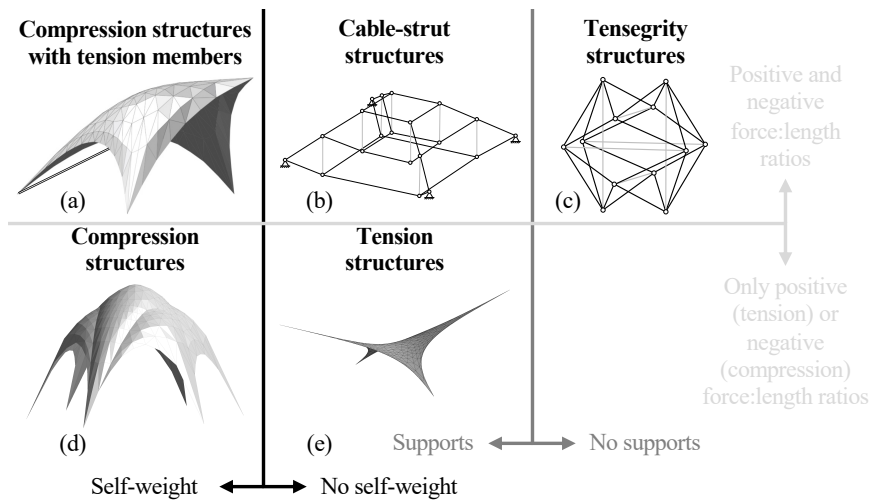


**Figure 1.** Examples of (a) compression structures with tension members (adapted from [29]), (b) cable-strut structures (adapted from [30]), (c) tensegrity structures, (d) compression structures and (e) tension structures.

## 2.2 Rank deficiency

In both tension (Figure 1.e) and compression (Figure 1.d) structures the corresponding

matrix  $\mathbf{D}$  is nonsingular and the form-finding problem is well-solved ([27] and [28] respectively). In compression structures with tension members matrix  $\mathbf{D}$  can be singular and some additional conditions must be taken into account regarding its condition number [29].

In the case of tensegrity structures and according to the definition of  $\mathbf{D}$ , the sum of the elements of each row or column of  $\mathbf{D}$  is zero. Due to this, matrix  $\mathbf{D}$  in tensegrity structures is always singular and special considerations have to be taken into account in the form-finding process. The non-degeneracy condition of tensegrity structures states that in order to obtain a tensegrity of dimension  $d$ , it is necessary that its corresponding matrix  $\mathbf{D}$  must have a rank deficiency of at least  $d + 1$  [14,18]. The rank-nullity theorem of linear algebra states that the rank plus the nullity of a matrix is equal to its number of columns. The nullity of a matrix corresponds with the dimension of  $\ker(\mathbf{D})$ . As  $\ker(\mathbf{D})$  is the eigenspace of eigenvalue 0, the dimension of  $\ker(\mathbf{D})$  coincides with the multiplicity of the eigenvalue 0. Consequently, in order to obtain a tensegrity structure of dimension  $d$ , the multiplicity of the eigenvalue 0 of  $\mathbf{D}$  must be at least  $d + 1$ .

The force density matrix  $\mathbf{D}$  is a symmetric real matrix due to its definition ( $\mathbf{D} = \mathbf{C}^T \mathbf{Q} \mathbf{C}$ ) and, according to the spectral theorem, it is orthogonally diagonalizable:  $\mathbf{A} = \mathbf{P}^{-1} \mathbf{D} \mathbf{P}$ . The diagonal matrix  $\mathbf{A}$  contains all the eigenvalues of  $\mathbf{D}$  ( $\lambda_1, \dots, \lambda_n$ ) and  $\mathbf{P}$  is an orthogonal matrix (that is,  $\mathbf{P}^{-1} = \mathbf{P}^T$ ) where its columns are an orthonormal base of eigenvectors of  $\mathbf{D}$ . The eigenvalues of  $\mathbf{D}$  are the solutions of the characteristic polynomial  $p(\lambda) = \lambda^n + a_{n-1} \lambda^{n-1} + \dots + a_1 \lambda + a_0$ . As in tensegrity structures the sum of the elements of each row or column of  $\mathbf{D}$  is zero,  $a_0 = 0$  [18]. Coefficients  $a_{n-1}, \dots, a_1$  are expressed in terms of the force:length ratio of all the members of the tensegrity. In order to obtain a three-dimensional tensegrity ( $d = 3$ ), the eigenvalue 0 must have at least a multiplicity of 4 and consequently coefficients  $a_3, a_2$  and  $a_1$  of the characteristic polynomial must be 0. The

previous condition leads to the system of equations shown in Eq. (2), which can be solved analytically if some relations between  $q$  values are imposed. These imposed conditions are based on symmetry and/or topology.

$$\left. \begin{aligned} a_3(q_1, \dots, q_m) &= 0 \\ a_2(q_1, \dots, q_m) &= 0 \\ a_1(q_1, \dots, q_m) &= 0 \end{aligned} \right\} \quad (2)$$

A more detailed description of the analytical form-finding procedure used in the work can be seen in [18,20].

### 2.3 Super-stability of tensegrity structures

A tensegrity is considered to be stable if it returns to its equilibrium configuration after release of small enforced deformations. The stability of tensegrity structures has been discussed in detail in [20,33,34]. In this work the super-stability criterion of tensegrity structures has been adopted. A tensegrity is called super-stable if it is always stable, regardless its prestress and material properties [34,35]. The super-stability conditions of tensegrities are [33–35]:

- i. The rank deficiency of the force density matrix  $\mathbf{D}$  is exactly  $d + 1$ .
- ii. The force density matrix  $\mathbf{D}$  is positive semi-definite.
- iii. The rank of the geometry matrix  $\mathbf{G}$  is  $(d^2 + d)/2$ .

The definition of the geometry matrix  $\mathbf{G}$  can be seen in [33].

### 3. Tensegrity families and truncated regular polyhedral tensegrities: topological and geometrical construction of tensegrity structures

Tensegrity structures can be constructed by assembling elementary cells [36,37]. In Pugh [36] two patterns are identified (among others): the diamond and the zigzag patterns. In the diamond pattern cables form diamonds or rhombic cells with a strut defining one

diagonal (see Figure 2.a). In the case of the zigzag pattern, an opposite pair of cables of a diamond cell are removed and a new cable is added in such a way that form a Z shape between the ends of the strut (see Z-shaped cell in Figure 2.b).

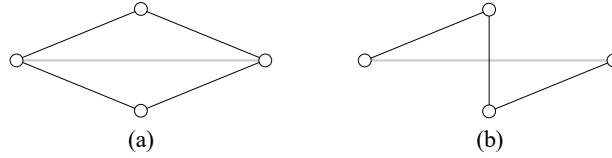


**Figure 2. Diamond or rhombic (a) and zigzag or Z-shaped (b) elementary cells (black and grey lines correspond to cables and struts respectively).**

### 3.1 Tensegrity families. The octahedron family

A group of tensegrity structures that share a common connectivity pattern forms a tensegrity family [20]. The octahedron family is composed by the octahedron, the expanded octahedron and the double-expanded octahedron [20]. The first member of the family (the octahedron in Figure 3.a) is composed by 12 cables, 3 struts and 6 nodes that conform 3 rhombic cells [20]. The second member is the expanded octahedron (see Figure 3.b), which is composed by 24 cables, 6 struts and 12 nodes that conform 6 rhombic cells [20]. The expanded octahedron comes from the expansion of the octahedron, by duplicating all its members and nodes following the topological rules of the family. In addition, it was demonstrated that the octahedron is a folded form the expanded octahedron [20]. Finally, the third component of the octahedron family (the double expanded-octahedron, see Figure 3.c) was obtained in [20] from the expansion of the expanded octahedron taking into consideration the particular topological rules of the family. The double-expanded octahedron has 48 cables, 12 struts and 24 nodes that conform 12 rhombic cells [20]. In the three members of the octahedron family shown in Figure 3 only two possible values of  $q$  were considered: cables and struts.

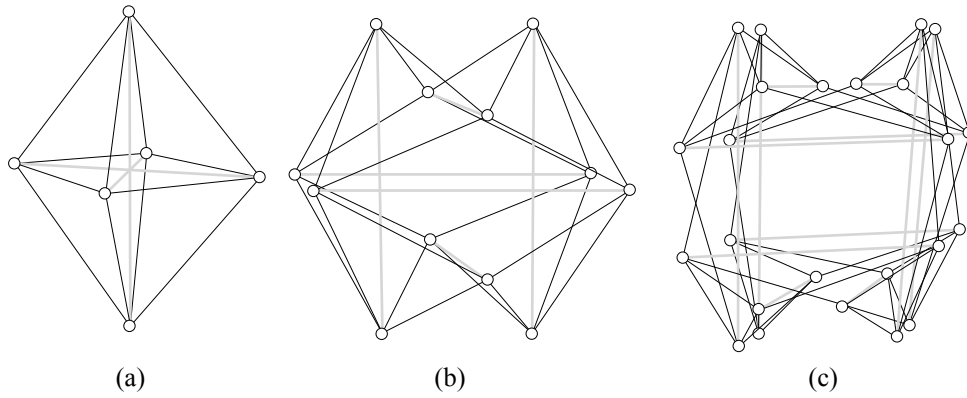


**Figure 3. Members of the octahedron family: the octahedron (a), the expanded-octahedron (b) and the double-expanded octahedron (c). Black and grey lines correspond to cables and struts respectively.**

Tensegrity families can be considered as a great source of new tensegrity forms whose members are obtained based on topology. These new forms can be obtained either from an expansion process or by introducing a higher number of different force:length ratio values for both cables and struts.

### 3.2 Truncated regular polyhedral tensegrities

Truncated regular polyhedral tensegrities are tensegrity structures defined geometrically from truncated regular polyhedrons [19,24,25]. Nodes in this type of tensegrities coincide with the vertices of a truncated polyhedron. Then tensegrities are constructed following the procedure proposed by Li et al. [37]. Let us consider the truncated tetrahedron shown in Figure 4.a as an example. In a truncated regular tetrahedral tensegrity each cable corresponds with an edge of the truncated tetrahedron (see Figure 4.b). The struts connect some vertices following the pattern of the Z-shaped elementary cells proposed in [37]. In Figure 4.b only a Z-shaped cell is depicted. The diamond or rhombic truncated tetrahedron can be constructed from a Z-based one simply by replacing Z-shaped cells with rhombic cells (see Figure 4.c). As in Figure 4.b, in Figure 4.c only a rhombic cell is represented for the sake of clarity of the figure. Similarly, rhombic truncated tetrahedral, cubic, octahedral, dodecahedral and icosahedral tensegrities can be obtained following

the same rules (see [19]).

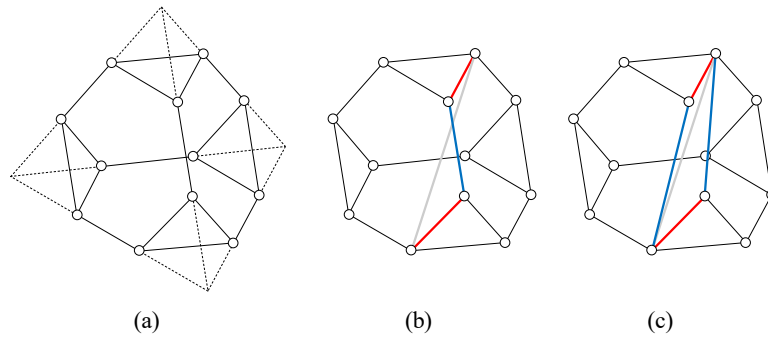


**Figure 4. (a) Truncated regular tetrahedron, (b) connectivity rules of the truncated regular tetrahedral tensegrity and (c) connectivity rules of the rhombic truncated tetrahedron. In (b) and (c) only a Z-shaped cell and a rhombic cell are drawn. Red, blue and gray lines correspond to type 1 cables, type 2 cables and struts, respectively. (For interpretation of the references to color in this figure legend, the reader is referred to the web version of this article).**

It is obvious that the number of cables in a rhombic tensegrity is higher than in a Z-based tensegrity. As can be seen in Figure 4.b and 2.c the cables of truncated tensegrities constructed by both elementary rhombic or Z-based cells can be grouped into two types: type 1 (truncating cables) and type 2 (remaining cables). So, each Z-shaped cell consists of two type 1 cables and one type 2 cable while each rhombic cell consists of two cables of both type 1 and type 2.

#### **4. The Z-octahedron family: a new family of tensegrity structures**

All the members of the octahedron family presented in [20] were formed by rhombic cells. In this piece of work, a new tensegrity family (the Z-octahedron family) is defined replacing the rhombic cells with Z-shaped cells. In addition, a higher number of possible values of  $q$  is considered.

##### **4.1 The Z-octahedron**

Figure 5 shows the plane connection graph of both the Z-octahedron (a) and the octahedron (b). A plane connection graph is a graphical representation of the connectivity between the nodes of a tensegrity structure [20] and it is defined following certain

topological rules, which are specific for each family (in the case of Figure 5.b, the octahedron family [20]).

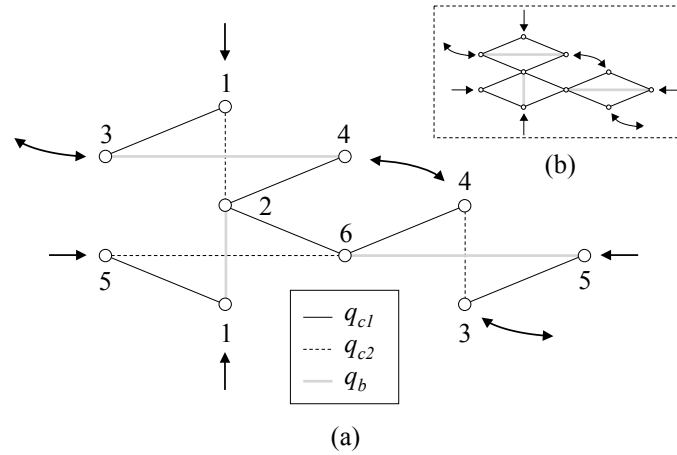


**Figure 5. Plane connection graph of the Z-octahedron (a) and of the octahedron (adapted from [20]) (b).**

Diamond cells of the octahedron (Figure 5.b) are replaced by Z-shaped cells in order to obtain the plane connection graph of the Z-octahedron (Figure 5.a). In the form-finding process of the octahedron carried out in [20] it was considered that all the struts and ties have the same force:length ratio value respectively. In this work three different values of force:length ratio are going to be considered in the definition of the Z-octahedron family:  $q_{c1}$  for type-1 cables (continuous black lines in Figure 5.a),  $q_{c2}$  for type-2 cables (dashed black lines in Figure 5.a) and  $q_b$  for struts (grey lines in Figure 5.a). Type-1 and type 2 cables have been identified following the rule of the Z-shaped elementary cell depicted in Figure 4.b.

The plane connection graph shown in Figure 5.a proves that the construction of the Z-octahedron is impossible and so it does not exist. Note that there are members that are simultaneously defined as both strut and cable (see, for example, the two members connecting nodes 1 and 2 in Figure 5.a).

## 4.2 The Z-expanded octahedron

The plane connection graph of the Z-expanded octahedron can be seen in Figure 6.a. As in the previous case, it has been constructed based on the plane connection graph of the second member of the octahedron family (i.e. the expanded octahedron, see Figure 6.b) by replacing the rhombic cells by Z-shaped cells. The Z-expanded octahedron has 24 members (6 struts and 18 cables) and 12 nodes. The connectivity matrix  $\mathbf{C} \in \mathcal{R}^{24 \times 12}$  of the Z-expanded octahedron is defined based on its plane connection graph (see Figure 6.a).

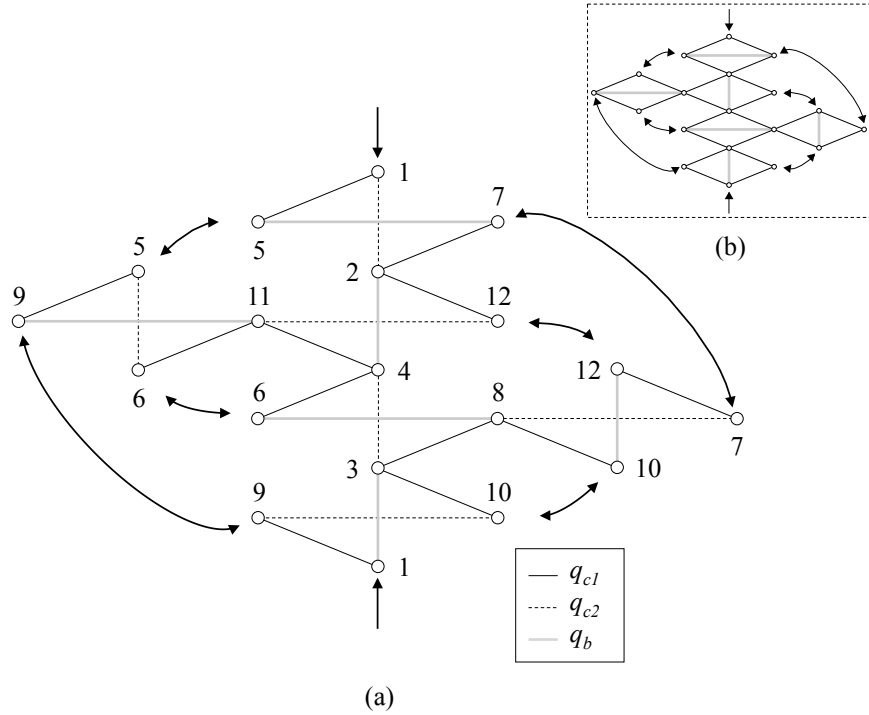


**Figure 6.** Plane connection graph of the Z-expanded octahedron (a) and of the expanded octahedron (adapted from [20]) (b).

Let us consider again three different values of  $q$ :  $q_{c1}$  for type-1 cables,  $q_{c2}$  for type-2 cables and  $q_b$  for struts (continuous black lines, dashed black lines and grey lines in Figure 6.a respectively), resulting in  $\mathbf{Q} \in \mathcal{R}^{24 \times 24}$ . Once matrices  $\mathbf{C}$  and  $\mathbf{Q}$  are defined, the force density matrix  $\mathbf{D} \in \mathcal{R}^{12 \times 12}$  is computed. Then the characteristic polynomial  $p(\lambda)$  of  $\mathbf{D}$  is computed and the non-degeneracy condition of a three dimensional tensegrity shown in Eq. (2) is imposed. For the sake of simplicity, two independent normalized force:length ratios taken as  $Q_1 = -q_{c1}/q_b > 0$  and  $Q_2 = -q_{c2}/q_b > 0$  are considered as in [19]. By doing

so, coefficients  $a_3$ ,  $a_2$  and  $a_1$  of  $p(\lambda)$  are expressed in terms of  $Q_1$  and  $Q_2$  (see Eqs. (A1), (A2) and (A3) of the Appendix A). The resultant system of equations  $a_1(Q_1, Q_2) = a_2(Q_1, Q_2) = a_3(Q_1, Q_2) = 0$  has the following solutions:  $\{q_b = 0\}$  (not considered),  $\{Q_1 = 0, Q_2 = 0\}$  (not considered),  $\{Q_1 = 0, Q_2 = 1\}$  (not considered),  $\{Q_1 = 1, Q_2 = -1\}$  (not possible because  $Q_2 < 0$ ) and the expressions shown in Eqs. (3) and (4).

$$Q_2 = \frac{-2 + 6Q_1 - 3Q_1^2 - \sqrt{4 - 8Q_1 + 8Q_1^2 - 12Q_1^3 + 9Q_1^4}}{4(-1 + Q_1)} \quad (3)$$

$$Q_2 = \frac{-2 + 6Q_1 - 3Q_1^2 + \sqrt{4 - 8Q_1 + 8Q_1^2 - 12Q_1^3 + 9Q_1^4}}{4(-1 + Q_1)} \quad (4)$$

All the equilibrium shapes of the Z-expanded octahedron considering three different values of  $q$  are collected in Eqs. (3) and (4). However, not all of them fulfill the super-stability conditions defined in Subsection 2.3. Hence, a study about the super-stability of the tensegrity forms resulting from Eqs. (3) and (4) must be carried out.

Figure 7.a shows the  $Q_1 - Q_2$  curves resulting from Eqs. (3) and (4). Firstly, the condition  $Q_1$  and  $Q_2 > 0$  is checked. If this condition is not fulfilled, cables have become struts or vice versa. According to this criterion, curve 1 of Eq. (4) and the part of the curve of Eq. (3) which is not in the region  $Q_1 > 0$  and  $Q_2 > 0$  must be excluded from the study. Secondly, condition (i) of the super-stability criterion is imposed, for which the rank deficiency of the resulting matrix  $\mathbf{D}$  must be exactly  $d+1$  (in this case 4). Tensegrity forms obtained from curve 2 of Eq. (4) and from the region  $Q_1 > 0$  and  $Q_2 > 0$  of Eq. (3) (which coincides with  $0 < Q_1 < 2/3$ ) have exactly 4 zero-eigenvalues. Thirdly, condition (ii) of the super-stability criterion is imposed, for which matrix  $\mathbf{D}$  must be positive semi-definite. Figure 7.b shows the minimum eigenvalue of matrix  $\mathbf{D}$  for all the  $Q_1 - Q_2$  pairs obtained from Eq. (3) in the region  $Q_1 > 0$  and  $Q_2 > 0$  considering  $q_c = -1$ . It can be seen from Figure 7.b that there is always a negative eigenvalue, so tensegrity forms resulting

from Eq. (3) do not fulfill condition (ii) of super-stability and they are excluded from the analysis. On the contrary, the matrix  $\mathbf{D}$  of the tensegrities obtained from curve 2 of Eq. (4) are always positive semi-definite. Finally, condition (iii) of the super-stability states that the rank of the geometry matrix  $\mathbf{G}$  must be  $(d^2 + d)/2 = 6$  (with  $d = 3$ , three-dimensional tensegrity). The tensegrity forms obtained from curve 2 of Eq. (4) have a geometry matrix with a rank of six. Consequently, all the  $Q_1 - Q_2$  pairs defined by curve 2 of Eq. (4) lead to tensegrity forms that fulfill all the super-stability conditions given in Section 2.3 and they can be considered as super-stable tensegrity structures.

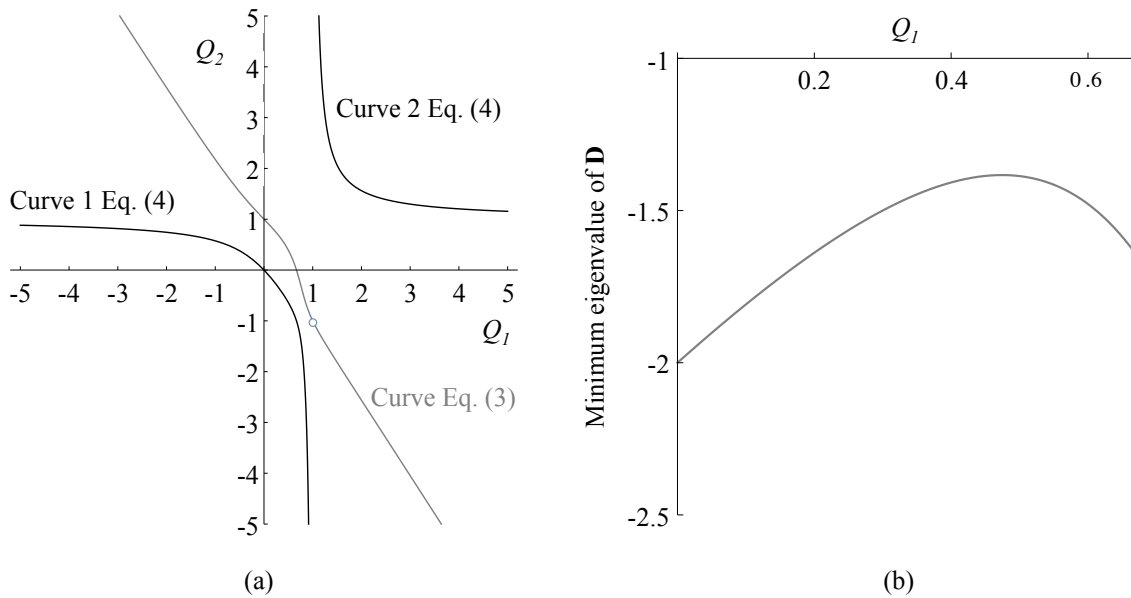


**Figure 7. (a)  $Q_1 - Q_2$  self-equilibrium curves of the Z-expanded octahedron (Eqs. (3) and (4)) and (b) minimum eigenvalue of  $\mathbf{D}$  for the  $Q_1 - Q_2$  curve of Eq. (3) in the region  $Q_1 > 0$  and  $Q_2 > 0$ .**

Figure 8 shows three equilibrium configurations of the Z-expanded octahedron considering different  $Q_1 - Q_2$  pairs of curve 2 of Eq. (4). It can be seen that, as  $Q_1$  increases in Eq. (4), the resultant tensegrity resembles more a truncated tetrahedron (see Figure 8). In [25] the truncated regular tetrahedral tensegrity is obtained by geometrical intuition based on a regular truncated tetrahedron and following the procedure proposed by Li et al. [37]. The connectivity of the nodes of this tensegrity coincides with the one of the Z-expanded octahedron (indicated in Figure 6.a) being the only difference that the

latter is obtained based only on topology. In Tibert and Pellegrino [9] an equilibrium configuration of a truncated tetrahedral tensegrity was defined:  $q_{s1} = 1$ ,  $q_{s2} = 1.3795$  and  $q_c = -0.6672$  (which corresponds with  $Q_1 = 1.499$  and  $Q_2 = 2.068$ ). This solution is in complete agreement with the analytical study presented in the work, because it corresponds to one of the  $Q_1 - Q_2$  pairs of curve 2 of Eq. (4). The solution obtained in Tibert and Pellegrino [9] is the one shown in Figure 8.a. If condition  $Q_1 = Q_2$  is imposed in Eq. (4), the analytical solution is  $Q_1 = Q_2 = (1 + \sqrt{41})/10$  (see Figure 8.b).

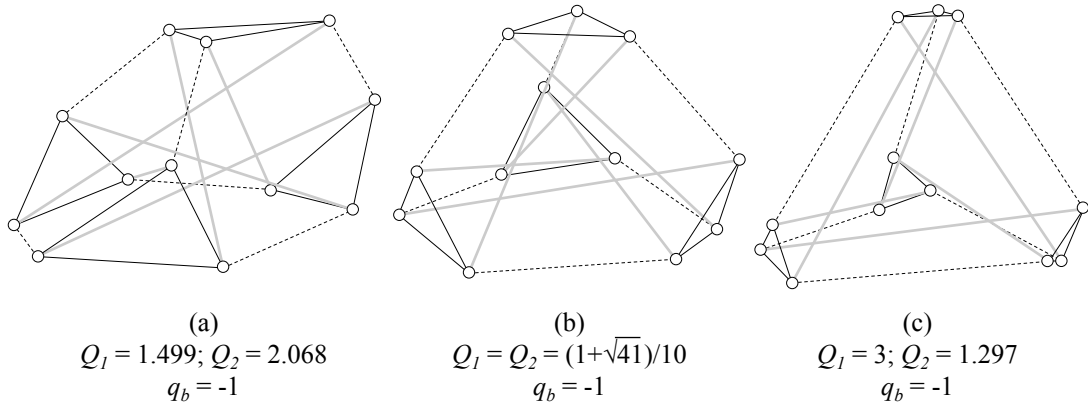


**Figure 8.** Equilibrium shapes of the Z-expanded octahedron obtained from the plane connection graph shown in Figure 6.a considering different values of  $q$ . (a)  $Q_1 = 1.499$  &  $Q_2 = 2.068$  (Eq. (4)) &  $q_b = -1$ , (b)  $Q_1 = (1 + \sqrt{41})/10$  &  $Q_2 = (1 + \sqrt{41})/10$  (Eq. (4)) &  $q_b = -1$  and (c)  $Q_1 = 3$  &  $Q_2 = 1.297$  (Eq. (4)) &  $q_b = -1$ . Black continuous and dashed lines and grey lines correspond to  $q_{c1}$ ,  $q_{c2}$  and  $q_b$  respectively in accordance with Figure 6.a.

### 4.3 The Z-double-expanded octahedron

The plane connection graph of the Z-double-expanded octahedron can be seen in Figure 9.a. It is constructed based on the plane connection graph of the double-expanded octahedron (see Figure 9.b) replacing the rhombic cells by Z-shaped cells. Consequently, the Z-double-expanded octahedron has 48 members (12 struts and 36 cables) and 24 nodes. As in the previous cases, the connectivity matrix of the Z-double-expanded octahedron  $\mathbf{C} \in \mathcal{R}^{48 \times 24}$  is constructed based on its plane connection graph (see Figure 9.a).

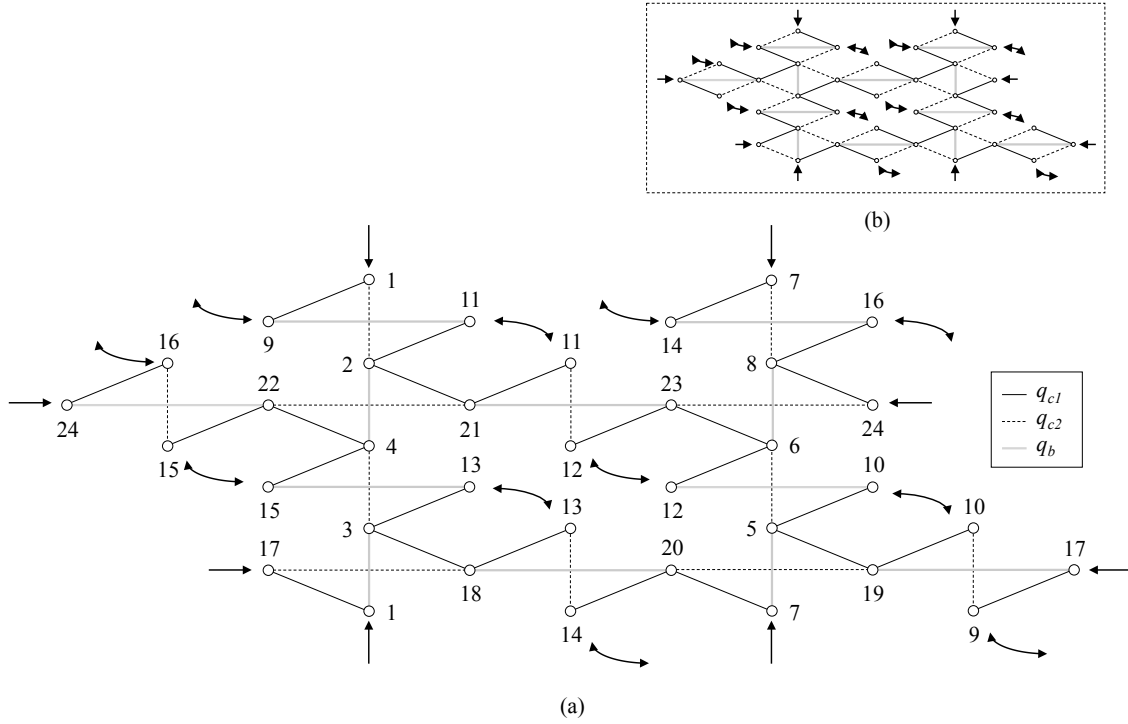


**Figure 9.** Plane connection graph of the Z-double-expanded octahedron (a) and of the double-expanded octahedron (adapted from [20]) (b).

Three different values of  $q$  are considered:  $q_{c1}$  for type-1 cables,  $q_{c2}$  for type-2 cables and  $q_b$  for struts (continuous black lines, dashed black lines and grey lines in Figure 9.a respectively), resulting in  $\mathbf{Q} \in \mathfrak{R}^{48 \times 48}$ . As in the previous case, matrix  $\mathbf{D} \in \mathfrak{R}^{24 \times 24}$  is computed and the coefficients  $a_3$ ,  $a_2$  and  $a_1$  of its corresponding characteristic polynomial  $p(\lambda)$  are expressed in terms of  $Q_1$  and  $Q_2$ . The expressions of  $a_1$  and  $a_2$  can be seen in Eqs. (A4) and Eq. (A5); the expression of  $a_3$  is not shown due to its length. The resultant system of equations  $a_1(Q_1, Q_2) = a_2(Q_1, Q_2) = a_3(Q_1, Q_2) = 0$  has the following solutions:  $\{q_b = 0\}$  (not considered),  $\{Q_1 = 0\}$  (not considered),  $\{Q_1 = 0, Q_2 = 1\}$  (not considered),  $\{Q_1 = 1, Q_2 = -1\}$  (not possible because  $Q_2 < 0$ ),  $\{Q_1 = 2/3, Q_2 = 0\}$  (not considered) and the expressions shown in Eqs. (3), (4) and (5).

$$Q_2 = \frac{3Q_1}{-4 + 3Q_1} \quad (5)$$

It can be noted that the solutions shown in Eqs. (3) and (4) are present in both the Z-

expanded octahedron and the Z-double-expanded octahedron. In this case Eqs. (3) and (4) correspond to a Z-expanded octahedron but with two nodes sharing the same position in the space (that is, duplicated nodes). This proves that the Z-expanded octahedron is a folded form of the Z-double-expanded octahedron and so they belong to the same family [20].

The next step is to study whether the superstability condition of the equilibrium configurations of the Z-double-expanded octahedrons collected in Eqs. (3), (4) and (5) is fulfilled. Figure 10.a shows the  $Q_1 - Q_2$  curves of the expressions shown in Eqs. (3), (4) and (5). First of all, the condition  $Q_1 > 0$  and  $Q_2 > 0$  is checked. Curve 2 of Eqs. (4) and (5) and the region  $0 < Q_1 < 2/3$  of Eq. (3) are the only solutions which fulfill this condition. So the rest of the curves are excluded from the analysis. Then the three super-stability conditions defined in Section 2.3 are checked. Condition (i) of the super-stability implies that the resulting matrix **D** must have 4 zero-eigenvalues in order to obtain a three-dimensional tensegrity. This condition is fulfilled by curve 2 of Eqs. (4) and (5) and by the region  $0 < Q_1 < 2/3$  of Eq. (3). Secondly, condition (ii) implies that the corresponding matrix **D** must be positive semi-definite. Figure 10.b shows the minimum eigenvalue of **D** corresponding to the  $Q_1 - Q_2$  pairs defined by curve 2 of Eqs. (4) and (5) and the region  $0 < Q_1 < 2/3$  of Eq. (3) considering  $q_c = -1$ . It can be seen that curve 2 of Eq. (4) and the region  $0 < Q_1 < 2/3$  of Eq. (3) always have a negative eigenvalue. As  $Q_1$  increases, the minimum eigenvalue of curve 2 of Eq. (4) approaches zero from the bottom and so the condition (ii) of the super-stability criterion is not fulfilled. Consequently, curve 2 of Eq. (4) and the region  $0 < Q_1 < 2/3$  of Eq. (3) are excluded from the analysis. Finally, condition (iii) of the super-stability criterion states that the rank of the geometry matrix **G** must be 6 (in the case of a three-dimensional tensegrity). The tensegrity forms obtained from curve 2 of Eq. (5) have a geometry matrix with a rank of six. Therefore, all the  $Q_1$

–  $Q_2$  pairs defined by curve 2 of Eq. (5) lead to a tensegrity form that fulfills all the super-stability conditions given in Section 2.3 and they can be considered as super-stable tensegrity structures.

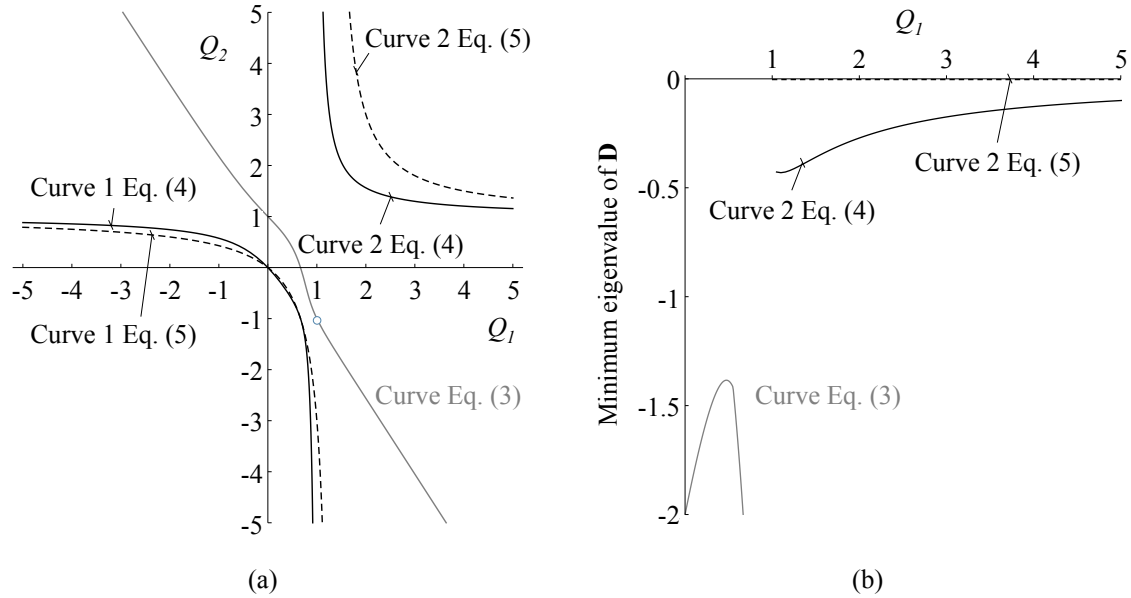


**Figure 10.** (a)  $Q_1 - Q_2$  self-equilibrium curves of the Z-double-expanded octahedron (Eqs. (3), (4) and (5)) and (b) minimum eigenvalue of  $D$  for the  $Q_1$ - $Q_2$  curves of Eqs. (3), (4) and (5) when both  $Q_1 > 0$  and  $Q_2 > 0$  are fulfilled.

Figure 11 shows some equilibrium configurations of the Z-double-expanded octahedron considering different  $q$  values according to Eq. (5). If condition  $Q_1 = Q_2$  is imposed in Eq. (5), the analytical solution  $Q_1 = Q_2 = 7/3$  is obtained (see Figure 11.b).

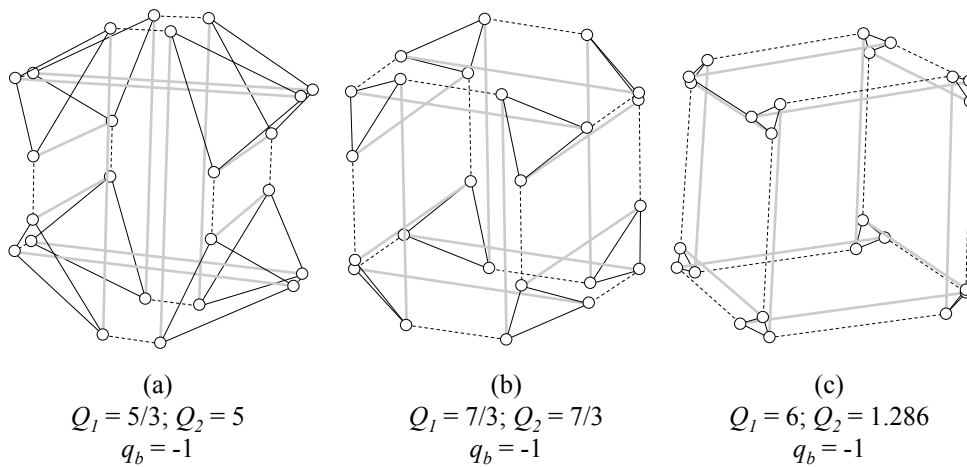


**Figure 11.** Equilibrium shapes of the Z-double-expanded octahedron obtained from the plane connection graph shown in Figure 9.a considering different values of  $q$ . (a)  $Q_1 = 5/3$  &  $Q_2 = 5$  (Eq. (5)) &  $q_b = -1$ , (b)  $Q_1 = 7/3$  &  $Q_2 = 7/3$  (Eq. (5)) &  $q_b = -1$  and (c)  $Q_1 = 6$  &  $Q_2 = 1.286$  (Eq. (5)) &  $q_b = -1$ .

Black continuous and dashed lines and grey lines correspond to  $q_{c1}$ ,  $q_{c2}$  and  $q_b$  respectively in accordance with Figure 9.a.

As can be seen in Figure 11, as  $Q_I$  increases in Eq. (5), the Z-double-expanded octahedron resembles more a truncated cube.

In [25] a truncated regular cubic tensegrity was defined by purely geometrical intuition following the procedure proposed by Li et al. [37]. However, the connectivity between the nodes of the tensegrity in [25] is not the same than the one of the Z-double-expanded octahedron represented in Figure 9.a. In both cases the cables coincide with the edges of the regular truncated cube but the connectivity of the struts is different. Figure 12.a and 12.b show the connectivity pattern of the struts of both the truncated regular cubic tensegrity [25] and the Z-double-expanded octahedron. As can be seen in Figure 12.c, struts in the Z-double-expanded octahedron connects nodes located in the same face of the polyhedron while, on the contrary, in the truncated regular cubic tensegrity [25] struts connect nodes located at different faces. It must be highlighted that the truncated regular cubic tensegrity [25] was defined by geometrical intuition, whereas the Z-double-expanded octahedron has been obtained from topology.

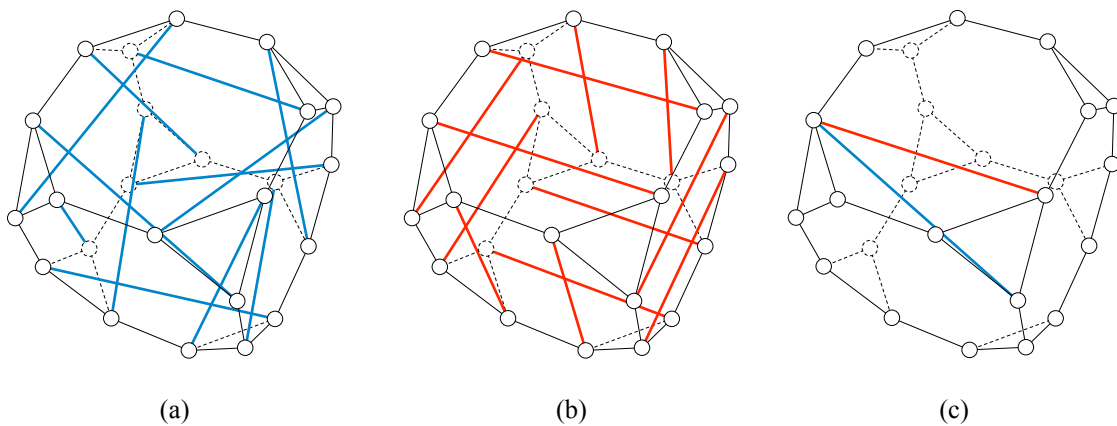


**Figure 12.** Truncated cube with: (a) strut connectivity of the truncated regular cubic tensegrity [25], (b) strut connectivity corresponding to the Z-double-expanded octahedron and (c) detail of the difference between (a) and (b).

## 5. Conclusions

A new tensegrity family is presented: the Z-octahedron family. The members of the family are constructed assembling Z-shaped elementary cells following its connectivity pattern. In particular, the rhombic cells of the members of the octahedron family (the octahedron, the expanded octahedron and the double-expanded octahedron) have been replaced by Z-shaped cells, leading to the definition of a new family. Consequently, it can be considered that the octahedron family presented in [20] is a good source of tensegrity forms.

In contrast with [20], where only two possible values of  $q$  were considered (cables and struts), in this work three different values of  $q$  are considered: one for struts and two for cables. An analytical analysis has been carried out during the form-finding process and super-stable tensegrity forms have been obtained. It has been demonstrated the inexistence of the Z-octahedron because for this particular case the connectivity pattern leads to some incongruences. However, the Z-expanded octahedron and the Z-double-expanded octahedron have been presented. The Z-double-expanded octahedron contains as folded forms all the equilibrium configurations of the Z-expanded octahedron, which is a necessary condition for tensegrity families.

It has been proved from topology that both the Z-expanded octahedron and the Z-double-expanded octahedron can also be obtained by purely geometrical intuition from a truncated regular tetrahedron and cube respectively.

### Appendix A. Polynomials $a_1$ , $a_2$ and $a_3$ .

For the Z-expanded octahedron presented in Section 4.2 the polynomials  $a_1$ ,  $a_2$  and  $a_3$  are the following:

$$a_1 = 576q_b^{11}Q_1^2 \left( 3Q_1^2(-1+Q_2) - 2(-1+Q_2)Q_2 + 2Q_1(1+(-3+Q_2)Q_2) \right)^3 \quad (A1)$$

$$a_2 = 48q_b^{10}Q_1 \left( 3Q_1^2(-1+Q_2) - 2(-1+Q_2)Q_2 + 2Q_1(1+(-3+Q_2)Q_2) \right)^2 \quad (A2)$$

$$\left( 81Q_1^3 + 168Q_1^2(-1+Q_2) - 16(-1+Q_2)Q_2 + 52Q_1(1+(-3+Q_2)Q_2) \right)$$

$$a_3 = 4q_b^9 \left( 3Q_1^2(-1+Q_2) - 2(-1+Q_2)Q_2 + 2Q_1(1+(-3+Q_2)Q_2) \right) \quad (A3)$$

$$\left( 2187Q_1^6 + 11664Q_1^5(-1+Q_2) + 64(-1+Q_2)^2 Q_2^2 - \right.$$

$$704Q_1(-1+Q_2)Q_2(1+(-3+Q_2)Q_2) + 96Q_1^3(-1+Q_2)$$

$$\left. \left( 80+Q_2(-267+80Q_2) \right) + 72Q_1^4(227+Q_2(-517+227Q_2)) + \right.$$

$$\left. \left. 16Q_1^2(67+(-1+Q_2)Q_2(612+Q_2(-545+67Q_2))) \right) \right)$$

For the Z-double-expanded octahedron presented in Section 4.3 the polynomials  $a_1$ ,  $a_2$  and  $a_3$  are the following:

$$a_1 = 9216q_b^{23}Q_1^5 \left( 3Q_1(-1+Q_2) - 4Q_2 \right)^3 (-1+Q_2)(-2+3Q_1+2Q_2)^2 \quad (A4)$$

$$\left( 3Q_1^2(-1+Q_2) - 2(-1+Q_2)Q_2 + 2Q_1(1+(-3+Q_2)Q_2) \right)^3$$

$$a_2 = 768q_b^{22}Q_1^4 \left( 3Q_1(-1+Q_2) - 4Q_2 \right)^2 (-2+3Q_1+2Q_2) \quad (A5)$$

$$\left( 3Q_1^2(-1+Q_2) - 2(-1+Q_2)Q_2 + 2Q_1(1+(-3+Q_2)Q_2) \right)^2$$

$$\left( 2349Q_1^5(-1+Q_2)^2 + 416(-1+Q_2)^3 Q_2^2 + \right.$$

$$1134Q_1^4(-1+Q_2)(5+Q_2(-12+5Q_2)) -$$

$$16Q_1(-1+Q_2)^2 Q_2(86+Q_2(-273+86Q_2)) +$$

$$24Q_1^2(-1+Q_2) \left( 37+Q_2(-393+Q_2(774+Q_2(-393+37Q_2))) \right) \right) +$$

$$36Q_1^3 \left( 113+Q_2(-651+Q_2(1080+Q_2(-651+113Q_2))) \right) \right)$$

## References

- [1] Fuller RB. Synergetics - explorations in the geometry of thinking. London, UK: Macmillan; 1975.

- [2] Ingber DE. Tensegrity I. Cell structure and hierarchical systems biology. *J Cell Sci* 2003;116:1157–73. doi:10.1242/jcs.00359.
- [3] Ingber DE. Cellular tensegrity: defining new rules of biological design that govern the cytoskeleton. *J Cell Sci* 1993;104 ( Pt 3:613–27.
- [4] Tibert AG, Pellegrino S. Deployable Tensegrity Reflectors for Small Satellites. *J Spacecr Rockets* 2002;39:701–9. doi:10.2514/2.3867.
- [5] Graells Rovira A, Mirats Tur JM. Control and simulation of a tensegrity-based mobile robot. *Rob Auton Syst* 2009;57:526–35. doi:10.1016/j.robot.2008.10.010.
- [6] Rhode-Barbarigos L, Hadj Ali NB, Motro R, Smith IFC. Designing tensegrity modules for pedestrian bridges. *Eng Struct* 2010;32:1158–67. doi:10.1016/j.engstruct.2009.12.042.
- [7] Feron J, Boucher L, Denoël V, Latteur P. Optimization of Footbridges Composed of Prismatic Tensegrity Modules. *J Bridg Eng* 2019;24. doi:10.1061/(ASCE)BE.1943-5592.0001438.
- [8] Yin X, Gao ZY, Zhang S, Zhang LY, Xu GK. Truncated regular octahedral tensegrity-based mechanical metamaterial with tunable and programmable Poisson's ratio. *Int J Mech Sci* 2020;167:105285. doi:10.1016/j.ijmecsci.2019.105285.
- [9] Tibert AG, Pellegrino S. Review of Form-Finding Methods for Tensegrity Structures. *Int J Sp Struct* 2003;18:209–23. doi:10.1260/026635103322987940.
- [10] Linkwitz K, Schek HJ. Einige Bemerkungen zur Berechnung von vorgespannten Seilnetzkonstruktionen. *Ingenieur-Archiv* 1971;40:145–58. doi:10.1007/BF00532146.
- [11] Schek HJ. The force density method for form-finding and computation of general networks. *Comput Methods Appl Mech Eng* 1974;3:115–34. doi:10.1016/0045-

- 7825(74)90045-0.
- [12] Tran HC, Lee J. Advanced form-finding of tensegrity structures. *Comput Struct* 2010;88:237–46. doi:10.1016/j.compstruc.2009.10.006.
- [13] Vassart N, Motro R. Multiparametered form-finding method: application to tensegrity systems. *Int J Sp Struct* 1999;14:89–104.
- [14] Zhang JY, Ohsaki M. Adaptive force density method for form-finding problem of tensegrity structures. *Int J Solids Struct* 2006;43:5658–73. doi:10.1016/j.ijsolstr.2005.10.011.
- [15] Otter JRH. Computations for prestressed concrete reactor pressure vessels using dynamic relaxation. *Nucl Struct Eng* 1965;1:61–75. doi:10.1016/0369-5816(65)90097-9.
- [16] Motro R. Forms and forces in tensegrity systems. In: Nooshin H, editor. *Proc. Third Int. Conf. Sp. Struct.*, Amsterdam: Elsevier; 1984, p. 180–5.
- [17] Bel Hadj Ali N, Rhode-Barbarigos L, Smith IFC. Analysis of clustered tensegrity structures using a modified dynamic relaxation algorithm. *Int J Solids Struct* 2011;48:637–47. doi:10.1016/j.ijsolstr.2010.10.029.
- [18] Hernández-Montes E, Fernández-Ruiz MA, Gil-Martín LM, Merino L, Jara P. Full and folded forms: a compact review of the formulation of tensegrity structures. *Math Mech Solids* 2018;23:944–9. doi:10.1177/1081286517697372.
- [19] Zhang LY, Li Y, Cao YP, Feng XQ. A unified solution for self-equilibrium and super-stability of rhombic truncated regular polyhedral tensegrities. *Int J Solids Struct* 2013;50:234–45. doi:10.1016/j.ijsolstr.2012.09.024.
- [20] Fernández-Ruiz MA, Hernández-Montes E, Carbonell-Márquez JF, Gil-Martín LM. Octahedron family: The double-expanded octahedron tensegrity. *Int J Solids Struct* 2019;165:1–13. doi:10.1016/j.ijsolstr.2019.01.017.

- [21] Estrada GG, Bungartz H-J, Mohrdieck C. Numerical form-finding of tensegrity structures. *Int J Solids Struct* 2006;43:6855–68.
- [22] Xu X, Wang Y, Luo Y. Finding member connectivities and nodal positions of tensegrity structures based on force density method and mixed integer nonlinear programming. *Eng Struct* 2018;166:240–50.  
doi:10.1016/j.engstruct.2018.03.063.
- [23] Cai J, Feng J. Form-finding of tensegrity structures using an optimization method. *Eng Struct* 2015;104:126–32. doi:10.1016/j.engstruct.2015.09.028.
- [24] Zhang JY, Ohsaki M. Self-equilibrium and stability of regular truncated tetrahedral tensegrity structures. *J Mech Phys Solids* 2012;60:1757–70.  
doi:10.1016/j.jmps.2012.06.001.
- [25] Zhang LY, Li Y, Cao YP, Feng XQ, Gao H. Self-equilibrium and super-stability of truncated regular polyhedral tensegrity structures: A unified analytical solution. *Proc R Soc A Math Phys Eng Sci* 2012;468:3323–47.  
doi:10.1098/rspa.2012.0260.
- [26] Hernández-Montes E, Jurado-Piña R, Bayo E. Topological Mapping for Tension Structures. *J Struct Eng* 2006;132:970–7. doi:10.1061/(ASCE)0733-9445(2006)132:6(970).
- [27] Hernández-Montes E, Jurado-Piña R, Bayo E. Topological Mapping for Tension Structures. *J Struct Eng* 2006;132:970–7. doi:10.1061/(ASCE)0733-9445(2006)132:6(970).
- [28] Fernández-Ruiz MA, Hernández-Montes E, Carbonell-Márquez JF, Gil-Martín LM. Patterns of force:length ratios for the design of compression structures with inner ribs. *Eng Struct* 2017;148:878–89. doi:10.1016/j.engstruct.2017.07.027.
- [29] Fernández-Ruiz MA, Moskaleva A, Gil-Martín LM, Palomares A, Hernández-

- Montes E. Design and form- finding of compression structures with prestressing tendons. *Eng Struct* 2019;197:109394. doi:10.1016/j.engstruct.2019.109394.
- [30] Pellegrino S. A class of tensegrity domes. *Int J Sp Struct* 1992;7:127–42. doi:10.1177/026635119200700206.
- [31] Levy MP. The Georgia Dome and beyond: Achieving lightweight-longspan structures. *Spat. lattice Tens. Struct. Proc. IASS-ASCE*, New York: 1994, p. 560–2.
- [32] Wu M, Sasaki M. Structural behaviors of an arch stiffened by cables. *Eng Struct* 2007;29:529–41. doi:10.1016/j.engstruct.2006.05.018.
- [33] Zhang JY, Ohsaki M. *Tensegrity Structures. Form, Stability, and Symmetry*. Springer; 2015.
- [34] Zhang JY, Ohsaki M. Stability conditions for tensegrity structures. *Int J Solids Struct* 2007;44:3875–86. doi:10.1016/j.ijsolstr.2006.10.027.
- [35] Connelly R. Tensegrity structures. Why are they stable? In: Thorpe MF, Duxbury PM, editors. *Rigidity theory Appl.*, Kluwer Academic / Plenum Publishers; 1998, p. 47–54.
- [36] Pugh A. *An introduction to tensegrity*. University of California Press: 1976.
- [37] Li Y, Feng XQ, Cao YP, Gao H. Constructing tensegrity structures from one-bar elementary cells. *Proc R Soc A Math Phys Eng Sci* 2010;466:45–61. doi:10.1098/rspa.2009.0260.